AD-A065 179 PENNSYLVANIA STATE UNIV UNIVERSITY PARK APPLIED RESE--ETC F/G 20/4
A SIMPLIFIED METHOD FOR PREDICTING BODY TEMPERATURE DISTRIBUTIO--ETC(U)
JAN 79 N00024-79-C-6043

UNCLASSIFIED TM-79-02 NL

1 OF 1
ADA
065179

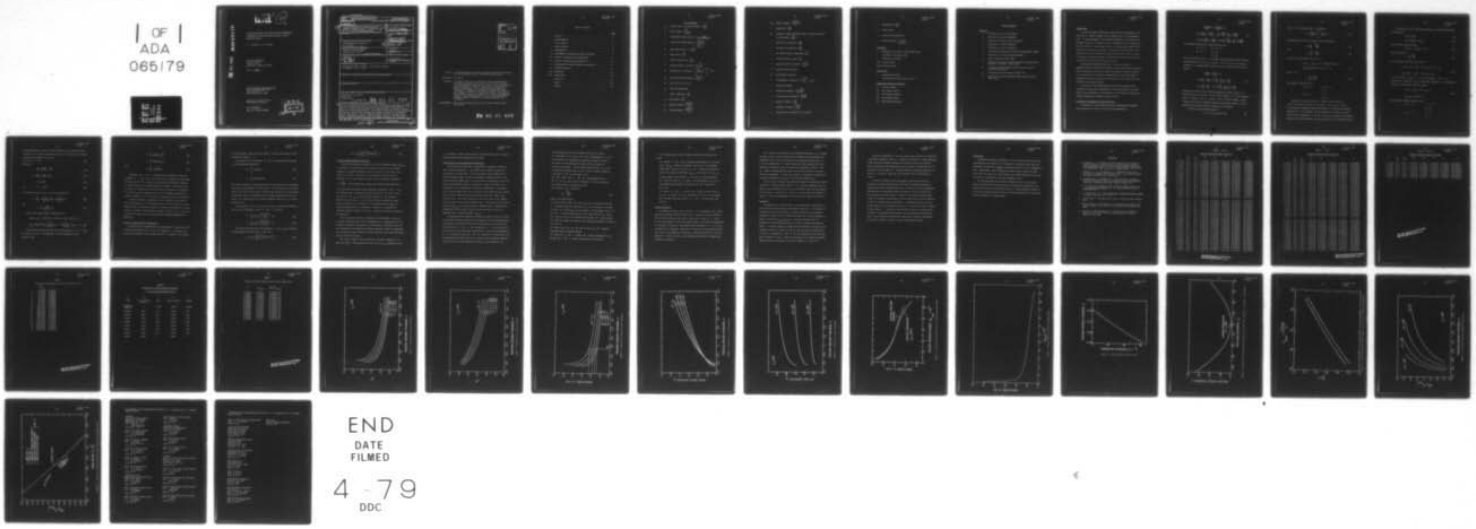

END
DATE
FILMED
4-79
DDC

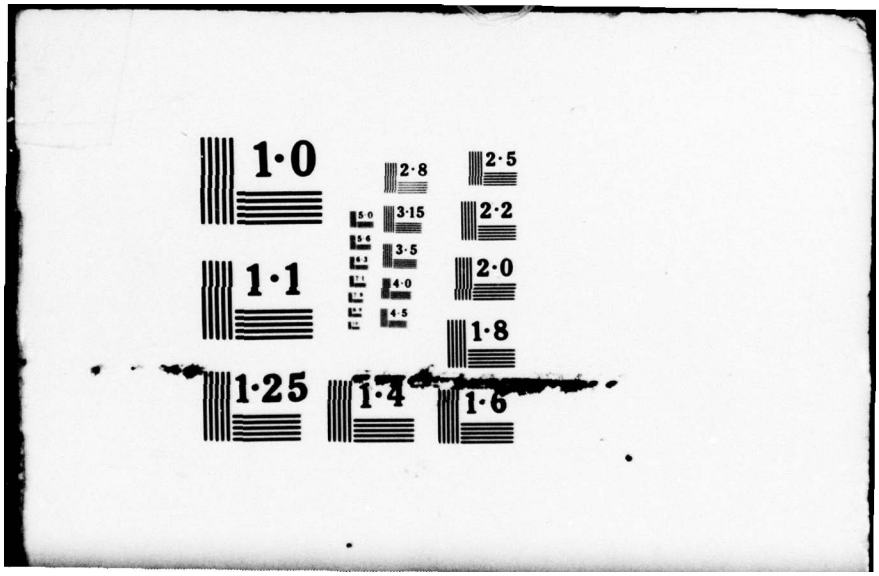
1·0
1·1
1·25
1·4
1·6
1·8
2·0
2·2
2·5
2·8
3·15
3·5
4·0
4·5

A SIMPLIFIED METHOD FOR PREDICTING BODY TEMPERATURE DISTRIBUTION IN THE PRELIMINARY DESIGN OF HEATED UNDERWATER BODIES

J. J. Eisenhuth, G. H. Hoffman

Technical Memorandum
File No. TM 79-02
4 January 1979
Contract No. N00024-79-C-6043

Copy No. 32

The Pennsylvania State University
APPLIED RESEARCH LABORATORY
Post Office Box 30
State College, PA 16801

NAVY DEPARTMENT
NAVAL SEA SYSTEMS COMMAND

UNCLASSIFIED

SECURITY CLASSIFICATION OF THIS PAGE *(When Data Entered)*

REPORT DOCUMENTATION PAGE

READ INSTRUCTIONS BEFORE COMPLETING FORM

1. REPORT NUMBER: TM-79-02	2. GOVT ACCESSION NO.
3. RECIPIENT'S CATALOG NUMBER	
4. TITLE (and Subtitle): A SIMPLIFIED METHOD FOR PREDICTING BODY TEMPERATURE DISTRIBUTION IN THE PRELIMINARY DESIGN OF HEATED UNDERWATER BODIES.	5. TYPE OF REPORT & PERIOD COVERED: Technical Memorandum
	6. PERFORMING ORG. REPORT NUMBER
7. AUTHOR(s)	8. CONTRACT OR GRANT NUMBER(s): N00024-79-C-6043
9. PERFORMING ORGANIZATION NAME AND ADDRESS: Applied Research Laboratory, P. O. Box 30, State College, PA 16801	10. PROGRAM ELEMENT, PROJECT, TASK AREA & WORK UNIT NUMBERS: 4 Jan 79
11. CONTROLLING OFFICE NAME AND ADDRESS: Naval Sea Systems Command, Washington, DC 20362, Codes 031 and 035	12. REPORT DATE: 01/04/79
	13. NUMBER OF PAGES: 39
14. MONITORING AGENCY NAME & ADDRESS *(if different from Controlling Office)*: 43p.	15. SECURITY CLASS. *(of this report)*: Unclassified
	15a. DECLASSIFICATION/DOWNGRADING SCHEDULE

16. DISTRIBUTION STATEMENT *(of this Report)*

Approved for public release. Distribution unlimited.
Per NAVSEA - Feb. 7, 1979.

17. DISTRIBUTION STATEMENT *(of the abstract entered in Block 20, if different from Report)*

18. SUPPLEMENTARY NOTES

19. KEY WORDS *(Continue on reverse side if necessary and identify by block number)*

temperature distribution
heated body
boundary layer

(AD-M053 254)

79 03 01 049

20. ABSTRACT *(Continue on reverse side if necessary and identify by block number)*

A previous effort in the prediction of body temperature distributions to stabilize the boundary layer flow has resulted in a methodology for doing this. Recently it was found that the number of parameters could be reduced by one by means of an affine transformation. The previous method has thus been simplified. In addition, the numerical computational method was changed to one based on Keller's box method. This has permitted greater accuracy and stability in certain computational regions. This memorandum reports on this more simple method and again presents information on laminar separation and transition.

DD FORM 1 JAN 73 1473 EDITION OF 1 NOV 65 IS OBSOLETE

391 007

UNCLASSIFIED

SECURITY CLASSIFICATION OF THIS PAGE *(When Data Entered)*

Subject: A Simplified Method for Predicting Body Temperature Distribution in the Preliminary Design of Heated Underwater Bodies

References: See page 21.

Abstract: A previous effort in the prediction of body temperature distributions to stabilize the boundary layer flow has resulted in a methodology for doing this. Recently it was found that the number of parameters could be reduced by one by means of an affine transformation. The previous method has thus been simplified. In addition, the numerical computational method was changed to one based on Keller's box method. This has permitted greater accuracy and stability in certain computational regions. This memorandum reports on this more simple method and again presents information on laminar separation and transition.

Acknowledgment: This work was sponsored by Naval Sea Systems Command, Codes 031 and 035.

Table of Contents

List of Symbols

C_p specific heat at constant pressure = $\dfrac{C_p^*}{C_{p^*\infty}}$

E Eckert number = $\dfrac{U_\infty^{*2}}{C_{p^*\infty} T_\infty^*}$

F transformed stream function = $\dfrac{\psi^*}{(\rho_\infty^* \mu_\infty^* x^* U_e^*)^{1/2}}$

f transformed stream function = $\dfrac{\psi(x,y)}{\left[\dfrac{2\xi}{R_e}\right]^{1/2}}$

g temperature ratio = $T = \dfrac{T^*}{T_\infty^*}$

H shape factor = $\dfrac{\delta^*}{\theta}$

k thermal conductivity = $\dfrac{k^*}{k_\infty^*}$

M pressure gradient parameter = $\dfrac{x}{U_e}\dfrac{dU_e}{dx}$

N transformed y coordinate = $\left(\dfrac{U_e^*}{\nu_\infty^* x^*}\right)^{1/2} \int_0^{y^*} \rho dy^*$

P_R free-stream Prandtl number = $\dfrac{C_{p_\infty}^* \mu_\infty^*}{k_\infty^*}$

q^* heat flux per unit area

q_c heat flux coefficient

r radius coordinate = $\dfrac{r^*}{L^*}$

r_o body radius = $\dfrac{r_o^*}{L^*}$

R_e Reynolds number = $\dfrac{U_\infty^* L^* \rho_\infty^*}{\mu_\infty^*}$

R_x Reynolds number = $\dfrac{U_e^* x^* \rho_\infty^*}{\mu_\infty^*}$

R_{δ^*} Reynolds number = $\dfrac{U_e^* \delta^* \rho_\infty^*}{\mu_\infty^*}$

T temperature = $\dfrac{T^*}{T_\infty^*}$

U_e velocity at edge of boundary layer = inviscid velocity at body surface = $\dfrac{U_e^*}{U_\infty^*}$

u velocity in x direction = $\dfrac{u^*}{U_\infty^*}$

v velocity in y direction = $\dfrac{v^*}{U_\infty^*}$

x arc length distance along body = $\dfrac{x^*}{L^*}$

y distance normal to body = $\dfrac{y^*}{L^*}$

β pressure gradient parameter = $\dfrac{2\xi}{U_e} \dfrac{dU_e}{d\xi}$

δ boundary layer thickness

δ^* displacement thickness

η transformed y coordinate = $\left(\dfrac{R_e}{2\xi} \right)^{1/2} U_e r_o dy$

θ momentum thickness

Λ Pohlhausen parameter = $\dfrac{\delta}{\nu_\infty^*} \dfrac{dU_e^*}{dx^*}$

λ radius gradient parameter = $\dfrac{2x}{r_o} \dfrac{dr_o}{dx}$

μ dynamic viscosity = $\dfrac{\mu^*}{\mu_\infty^*}$

ν kinematic viscosity = $\dfrac{\nu^* \rho_\infty^*}{\mu_\infty^*}$

ξ transformed x coordinate ($d\xi = U_e r_o^2 dx$)

ρ mass density = $\frac{\rho^*}{\rho_\infty^*}$

τ^* shear stress

τ_c shear stress coefficient

ψ stream function = $\frac{\psi}{\rho_\infty^* L^{*2} U_\infty^*}$

Subscripts

e evaluated at the edge of the boundary layer

∞ evaluated in the free stream

w evaluated at the wall

crit critical value

trans transition value

Superscripts

* dimensional quantity

' differentiation with respect to N or η

Dimensional Reference Quantities

L^* reference length

U_∞^* free-stream velocity

μ_∞^* free-stream viscosity

ρ_∞^* free-stream density

T_∞^* free-stream temperature

4 January 1979
JJE:pjk

List of Figures

Introduction

A recent ARL report (Reference 1) dealt with the calculation of the mean flow of a heated, laminar, water boundary layer on an axisymmetric body. In the development of the pertinent equations a coordinate transformation was used to eliminate explicit dependence on the coordinate in the flow direction. The computed velocity and temperature profiles were then given by similarity solutions. The detailed laminar boundry layer characteristics that resulted from these solutions were used as a means of developing a design procedure for specifying the distribution of wall temperature necessary to keep the flow stable.

Although the procedure worked well, the required number of parameters made the interpolation process that was used rather cumbersome and any presentation of data in tabular or graphical form was extensive. It is possible with a different transformation to reduce the number of parameters by one, thus reducing the complexity of the computations and ultimately the design procedure.

The details of the transformations used in both boundary layer computation methods and a description of the interrelation of the parameters will be presented. As in Reference 1, the effects of heating on laminar separation and transition will be given.

Development of Equations and Their Solutions

In Reference 1, for steady mean flow the incompressible boundary layer equations on a body of revolution were presented as:

$$\frac{\partial(\rho^* r^* u^*)}{\partial x^*} + \frac{\partial(\rho^* r^* v^*)}{\partial y^*} = 0$$

$$\rho^*\left(u^* \frac{\partial u^*}{\partial y^*} + v^* \frac{\partial u^*}{\partial y^*}\right) = \rho^* U_e^* \frac{dU_e^*}{dx^*} + \frac{\partial}{\partial y^*}\left(\mu^* \frac{\partial u^*}{\partial y^*}\right) \qquad (1)$$

$$\rho^* C_p^*\left(u^* \frac{\partial T^*}{\partial x^*} + v^* \frac{\partial T^*}{\partial y^*}\right) = -\rho^* u^* U_e^* \frac{dU_e^*}{dx^*} + \frac{\partial}{\partial y^*}\left(k^* \frac{\partial T^*}{\partial y^*}\right)$$

The boundary conditions for these equations are:

at $y^* = 0$ $\qquad u^* = v^* = 0$

as $y^* \to \infty$ $\qquad u^* \to U_e^*$

$\qquad\qquad\qquad\quad T^* \to T_\infty^*$

The third of Equations (1) is an energy balance equation in which buoyancy and dissipation by friction are ignored. The stars indicate dimensional quantities. In dimensionless terms (see List of Symbols), Equations (1) become:

$$\frac{\partial(\rho r u)}{\partial x} + \frac{\partial(\rho r v)}{\partial y} = 0$$

$$\rho\left(u \frac{\partial u}{\partial x} + v \frac{\partial u}{\partial y}\right) = \rho U_e \frac{dU_e}{dx} + \frac{1}{R_e} \frac{\partial}{\partial y}\left(\mu \frac{\partial u}{\partial y}\right) \qquad (2)$$

$$\rho C_p\left(u \frac{\partial T}{\partial x} + \frac{\partial T}{\partial y}\right) = -E\rho u U_e \frac{dU_e}{dx} + \frac{1}{P_R R_e} \frac{\partial}{\partial y}\left(k \frac{\partial T}{\partial y}\right)$$

Equations (1) and (2) do not include transverse curvature terms; i.e., derivatives of $r^*(= r_o^*(x^*) + y^* \cos\phi)$ with respect to y^* are considered small. In effect, then, $r^* = r_o^*(x^*)$. Also, the Eckert number, E, when evaluated for water at expected conditions in the free stream is a small quantity and the term in which it appears can be dropped.

A stream function can be defined as:

$$\psi = (\rho_\infty^* \mu_\infty^* x^* U_e^*)^{\frac{1}{2}} F(N) \qquad (3)$$

where N is the transformed y coordinate,

$$N = \left(\frac{U_e^*}{\nu_\infty^* x^*}\right)^{\frac{1}{2}} \int_0^{y^*} \left(\frac{\rho^*}{\rho_\infty^*}\right) dy^*. \tag{4}$$

Using Equations (3) and (4) along with the definitions:

$$M = \frac{x^*}{U_e^*} \quad \frac{dU_e^*}{dx^*} \tag{5}$$

and

$$\lambda = \frac{2\, x^*}{r_o^*} \quad \frac{dr_o^*}{dx^*}\,, \tag{6}$$

the last two of Equations (1) reduce to:

$$(\rho\mu F'')' + M\left(\frac{1}{\rho} - F'^2\right) + \left(\frac{M + \lambda + 1}{2}\right) FF'' = 0$$

$$P_R C_p \left(\frac{M + \lambda + 1}{2}\right) F\Theta' + (\rho k \Theta')' = 0 \tag{7}$$

where Θ is:

$$\Theta = \frac{T^* - T_\infty^*}{T_w^* - T_\infty^*} \tag{8}$$

The boundary conditions become:

at $N = 0$	$F' = F = 0$
	$\Theta = 1$
as $N \to \infty$	$F' \to 1$
	$\Theta \to 0$

Equations (7) were solved with a slightly altered scheme of Lowell and Reshotko presented in Reference 2. This scheme is based on the numerical integration process developed by Nachtscheim and Swigert (Reference 3). The procedure that was adopted was to assume a series of values for the parameter M, λ, and ΔT^* ($= T_w^* - T_\infty^*$), tabulate the calculated boundary layer characteristics, and use these results in a design procedure.

If Equations (2) are transformed according to the Mangler-Levy-Lees transformation,

$$d\xi = U_e r_o^2 dx \tag{9}$$

$$d\eta = (Re/2\xi)^{\frac{1}{2}} \; U_e r_o dy, \tag{10}$$

and a reduced stream function,

$$\psi(x,y) = (2\xi/R_e)^{\frac{1}{2}} \; f(\xi,\eta) \tag{11}$$

and the parameter,

$$\beta = \frac{2\xi}{U_e} \frac{dU_e}{d\xi} \tag{12}$$

are introduced, Equations (2) reduce to:

$$\begin{aligned} &(\rho\mu f'')' + ff'' + \beta(\frac{1}{\rho} - f'^2) = 2\xi(f'f'_\xi - f''f_\xi) \\ &\frac{1}{P_R}(\rho k g')' + C_p f g' = 2\xi C_p(f'g_\xi - g'f_\xi). \end{aligned} \tag{13}$$

g is used here in place of T. If the functions f and g are assumed to be independent of the transformed coordinate, ξ, the following similar-type homogeneous equations result:

$$\begin{aligned} &(\rho\mu f'')' + \beta(\frac{1}{\rho} - f'^2) + ff'' = 0 \\ &P_R C_p f g' + (\rho k g')' = 0. \end{aligned} \tag{14}$$

The attendant boundary conditions are:

at $\eta = 0$	$f = f' = 0$
	$g = T_w$
as $\eta \to \infty$	$f' \to 1$
	$g \to 1$

Although Equations (7) and (14) were derived by use of different transformations, their makeup suggests that they can be related with an affine transformation summarized as follows:

Set $F = Af, \quad \eta = BN.$ (15)

Therefore,

$$\frac{d}{dN} = \frac{d}{d\eta}\frac{d\eta}{dN} = B\frac{d}{d\eta}, \tag{16}$$

$$F' = \frac{dF}{dN} = AB\frac{df}{d\eta} = ABf', \tag{17}$$

$$F'' = AB^2 f'', \tag{18}$$

and

$$F''' = AB^3 f'''. \tag{19}$$

The relation between g and Θ can be developed with

$$\Theta' = \frac{d\Theta}{dN} = B\left(\frac{T_\infty^*}{T_w^* - T_\infty^*}\right)\frac{dg}{d\eta} = B\left(\frac{T_\infty^*}{T_w^* - T_\infty^*}\right)g' \tag{20}$$

and

$$\Theta'' = B^2\left(\frac{T_\infty^*}{T_w^* - T_\infty^*}\right)g''. \tag{21}$$

Making these substitutions in Equations (7),

$$(AB^3)(\rho\mu f'')' + \left(\frac{M+\lambda+1}{2}\right)(A^2P^2)ff'' + M\left(\frac{1}{\rho} - A^2B^2f'^2\right) = 0$$

$$P_R C_p \left(\frac{M+\lambda+1}{2}\right)(AB)\left(\frac{T_\infty^*}{T_w^* - T_\infty^*}\right)fg' + B^2\left(\frac{T_\infty^*}{T_w^* - T_\infty^*}\right)(\rho k g')' = 0 \tag{22}$$

From Equation (17) and the fact that in both systems $f' = F' = u/U_e$, it follows that $AB = 1$. Furthermore, to reduce Equations (22) to Equations (14),

$$A = \left[\frac{2}{M + \lambda + 1} \right]^{\frac{1}{2}}, \tag{23}$$

$$B = \left[\frac{M + \lambda + 1}{2} \right]^{\frac{1}{2}}, \tag{24}$$

and

$$\beta = \frac{M}{B^2} = \frac{2M}{M + \lambda + 1} \tag{25}$$

Therefore, the M and λ parameters can be combined to give one parameter, β. λ and M are, of course known for points on a given body from the details of its contour and the pressure distribution, measured or computed by way of the Douglas-Neumann procedure. The conclusion is, of course, that Equations (14) are basically the equivalent of Equations (7) and can be used to generate the data for the design procedure previously mentioned. In fact, solution of Equations (14) is less difficult.

A finite difference procedure due to H. B. Keller [4] was used in solving Equations (14). The procedure, known as the box method, was developed by Keller and applied successfully by Cebici and Smith [5] to a wide variety of problems. The physical properties of water, C_p, ρ, μ and k are a function of temperature and are known from information presented in Reference 2.

Results of Boundary Layer Computations

The boundary layer computations were performed for a parametric study in which the parameters were β and ΔT^* ($=T_w^*=T_\infty^*$). In all cases the free-stream temperature, T_∞^*, was kept at 60° F. A summary of the results

of this parameter study is found in Table 1. Plots of these data are also displayed in Figures 1 - 5.

The boundary layer thicknesses, δ^* and Θ, are defined in the sense of two-dimensional definitions,

$$\delta^* = \int_0^\infty (1-\rho^* u^*) dy \tag{26}$$

$$\Theta = \int_0^\infty \rho^* u^* (1-u^*) dy^*. \tag{27}$$

This leads eventually to slight differences when comparing with thicknesses resulting from axisymmetric considerations. Little difference in the shape factor, H (= δ^*/Θ), should result, however, when the point on the body under consideration has a small boundary layer thickness compared with the body radius. For considerations of a laminar boundary layer this is, of course, generally true.

The quantities, η_{δ^*} and η_Θ, given in Table 1 and shown in Figures 1 and 2, must be transformed to get δ^* and Θ as follows:

$$\delta^* = \left(\frac{2}{M + \lambda + 1}\right)^{\frac{1}{2}} \left(\frac{\nu_\infty^* x^*}{U_e^*}\right)^{\frac{1}{2}} \eta_{\delta^*} \tag{28}$$

$$\Theta = \left(\frac{2}{M + \lambda + 1}\right)^{\frac{1}{2}} \left(\frac{\nu_\infty^* x^*}{U_e^*}\right)^{\frac{1}{2}} \eta_\Theta \tag{29}$$

The shear stress and heat flux quantities, τ_c and q_c, must likewise be transformed as follows to get τ^* and q^*:

$$\tau^* = \mu_\infty U_e \left(\frac{U_e}{\nu_\infty x}\right)^{\frac{1}{2}} \left(\frac{M + \lambda + 1}{2}\right)^{\frac{1}{2}} \tau_c \tag{30}$$

$$q^* = k_\infty \left(\frac{U_e}{\nu_\infty x} \right)^{1/2} \left(\frac{M + \lambda + 1}{2} \right)^{1/2} q_c \qquad (31)$$

Critical Reynolds Number Correlation

Stability information in terms of the critical Reynolds number, $R_{\delta^*}{}_{crit}$ is available for two-dimensional flow both for the case of the unheated boundary with pressure gradient and for the flow over a flat plate with heating at the wall. The results of the unheated case are found in Reference 6 as critical Reynolds number versus the Pohlhausen parameter $\Lambda = \frac{\delta}{\nu} \frac{dU_e}{dx}$, and the heated case results were obtained from Reference 2 as critical Reynolds number versus temperature difference. The Λ and ΔT parameters were translated into the shape factor $H = \delta^*/\Theta$ so that in each case $R_{\delta^*}{}_{crit}$ could be plotted against H. The curves in Figure 6 are the result. It can be seen that the correlation is quite good, indicating that the stability of the laminar boundary layer is strongly dependent upon H, regardless of whether it is obtained by favorable pressure gradient or by heat. A similar correlation is reported in Reference 7.

This correlation provides the basis for the development of the type of design information which will be presented here. Although based on two-dimensional stability information, the correlation is considered valid for the axisymmetric case because the stability equations, under the assumption that the boundary layer thickness is small compared to the local body radius, are the same for both cases.

The curve in Figure 6 for the variation in pressure gradient is repeated in Figure 7 and extrapolated in the low $R_{\delta^*}{}_{crit}$ regardless of how

H is obtained. Table 2 gives specific values from this curve for ease in effecting computations involving these curves.

Determination of Body Temperature Distribution

The procedure outlined here is essentially a simplified version of that outlined in Reference 1. Two criteria were chosen to insure the maintenance of laminar flow: (1) the provision of just enough heat to keep the Reynolds number (based on displacement thickness) equal to the critical Reynolds number and, (2) the provision of enough heat so that the peak critical Reynolds number is maintained. These are referred to as "minimum heat" and "maximum heat" conditions respectively. The minimum heat criterion implies that, for a particular free-stream velocity, enough heat is added to make the operating Reynolds number R_δ^*, equal to the critical value. This should insure that there will never be any amplification of waves in the laminar boundary layer. The maximum heat criterion fixes the $R_{\delta^*_{crit}}$ at its maximum value. Whether there is amplification depends upon the free-stream velocity being high enough to have the operating R_δ^* exceed the maximum $R_{\delta^*_{crit}}$.

In implementing the temperature hunting procedure, the data in Table 1 can be filed and then recovered by the computer for interpolation purposes. The geometry and potential flow pressure distribution for a body will be known so that an M and a λ and, consequently, a β can be determined for each point on the body under consideration. This will be designated as β_o for a particular body point. The ΔT^* required at a body station can be determined by applying one of the criteria already mentioned and interpolating the data to get appropriate quantities corresponding to β_o.

In the minimum heat case the procedure would be as follows:

(1) Determine an H_o versus ΔT^* curve corresponding to β_o as illustrated by the interpolation procedure pictured in Figure 3. The curves can be represented by spline fits and values are extracted accordingly. All the other quantities (η_δ^*, q_c, τ_c) can be similarly handled so that a curve of each of these is known as a function of ΔT^* for particular β_o's.

(2) First choose $\Delta T^* = 0$. The η_δ^* corresponding then to $\Delta T^* = 0$ and β_o can be used to determine δ^* for a particular free-stream velocity using Equation (28).

(3) Calculate R_δ^* by means of

$$R_\delta^* = \frac{\delta^* U_e^*}{\nu_\infty^*} . \tag{31}$$

This is the operating R_δ^*.

(4) Enter Figure 7 with R_δ^* from step (3) to determine a required H. by entering with the operating R_δ^* we are saying that, in order for this to be the $R_{\delta^*_{crit}}$, we must produce a corresponding value of H.

(5) The H required from step (4) can be used with the H_o versus ΔT^* curve of step (1) to determine the required ΔT^*. This required ΔT^* now will change the value of η_δ^*, originally determined in step (2) for $\Delta T^* = 0$.

(6) Repeat steps (2), (3), (4), and (5) until the ΔT^* required converges within a desired accuracy.

(7) Enter the q_c and τ_c versus ΔT^* curves established for β_o and get the q and τ values from Equations (30) and (31).

For the maximum heat case the somewhat different procedure is as follows:

(1) Assume $H = 2.29$. This corresponds approximately to the point where $R_{\delta^*}{}_{crit}$ reaches its maximum. This is not a very precise number and it could be as low as $H = 2.2$. Adding heat beyond the value that produces the maximum $R_{\delta^*}{}_{crit}$ will result in $R_{\delta^*}{}_{crit}$ becoming smaller (see Reference 4) and thus be counterproductive.

(2) Enter the curve of H_o versus ΔT^*, determined in step (1) of the minimum heat procedure, and extract the ΔT^* required for $H_o = 2.29$.

(3) Extract q_c and τ_c for the ΔT^* of step (2) from curves of q_c and τ_c versus ΔT^* also determined in step (1) of the minimum heat procedure and again convert to q and τ via Equations (30) and (31).

Laminar Separation

An attempt was made to obtain limits of β for different ΔT^* values beyond which laminar separation would occur. Using the criterion that the skin friction vanishes at the point of separation, curves of τ_c versus β were extrapolated to obtain the desired limits. The computer program will not calculate a solution to the boundary layer equations at $\tau = 0$ so that extrapolation is necessary. Figure 8 is the result of those extrapolations. For a given local temperature difference, laminar separation will occur for values of β below the curve. The relatively small effect of temperature difference is apparent.

As a check on the accuracy of the calculated separation β, an attempt was made to get as close to separation as possible for the unheated two-dimensional case. This is the solution for Falkner-Skan Flows where β is now the Falkner-Skan β. These results were then compared with those presented in Reference 5 and the results are presented in Table 3. The f''_w values, representing the slope of the velocity profile at the wall, and the corresponding β values are compared. Richardson's extrapolation discussed in Reference 5 was used to get the ARL values of f''_w.

As can be seen, the Smith and ARL values compare favorably near laminar separation. The Keller-Cebeci Value of β at laminar separation does not appear to plot smoothly with the rest of the values listed and thus appears to be in error. A plot of f''_w versus β for the ARL results appears in Figure 9. Values corresponding to reverse flow also appear in this plot.

Transition

The prediction of transition for a given temperature distribution on a body follows the same lines as presented in Reference 1. The basis for the method used here is the plot of a band of calculated data supplied through the courtesy of A.M.O. Smith (See Figure 10). The band marks the range of values of $R_{x\ trans}$ versus H that were obtained from e^9 stabilitity calculations performed for a variety of heated and unheated wedges. It would be logical to choose the lower bound of this band as the transition criterion. Values for such a curve are given in tubular form in Table 4. Translating H into β for this transition curve, the plots shown in Figure 11 result. These curves indicate the transition Reynolds number that would correspond to particular values of β and ΔT^*.

As stated in Reference 1, the curve used as the criterion for transition is generally optimistic, that is, it predicts transition at a higher Reynolds number than some available unheated body transition data would indicate. This is evidenced by the experimental points plotted in comparison with the transition curve in Figure 12. The data points are taken from Reference 8. and the H values for these data were obtained from the information in Table 1.

In work not reported in this memorandum, correlation between the Transition Analysis Program System, TAPS, and the information from this similar type solution indicates that the H values for a given temperature distribution are consistantly higher for TAPS by a factor of about 1.03. This correlation is with respect to bodies of the type that would produce fairly flat pressure distributions and which would profit from the addition of heat for boundary layer stabilization. A suggested approach for estimating whether or not transition will occur is to replot the curve of Figure 12 with values of H reduced by 1.03 and then, using the calculated data of Table 3 in establishing the boundary layer characteristics, one would have a curve consistent with TAPS and experimental transition information. The curves of Figure 11 could, of course, be similarly altered.

Conclusions

Techniques developed in Reference 1 have been simplified and data have been generated that permit one to estimate in a relatively easy manner the temperature distribution necessary to stabilize the flow over an axisymmetric body. Additionally, these techniques and data provide a means for determining the local heat flux, skin friction, the laminar separation point, and the point of transition for a heated axisymmetric body.

All these estimates can be made by using the values of the various quantities presented in the tables and by following the interpolative procedures and criteria that have been outlined. A simple computer program to do this can be easily written or one can interpolate between the curves that are also included in this memorandum.

References

1. Eisenhuth, J. J., "Prediction of Body Temperature Distribution, Laminar Separation, and Transition in the Preliminary Design of Heated Underwater Bodies", TM 78-39, Applied Research Laboratory, The Pennsylvania State University, 22 February 1978. A053254

2. Lowell, R. L., Jr. and Reshotko, E., "Numberical Study of the Stability of a Heated, Water Boundary Layer," Case Western Reserve University, FTAS TR 73-93, January 1974.

3. Nachtsheim, P. R. and Swigert, P., "Satisfaction of Asymptotic Boundary Conditions in Numerical Solution of Systems of Nonlinear Equations of Boundary-Layer Type," NASA TN D-3004, 1965.

4. H. B. Keller, Some Computational Problems in Boundary Layer Flow, in Lecture Notes in Physics, Vol. 35, (Springer-Verlag, Berlin, 1975), pp. 1-21.

5. T. Cebeci and A. M. O. Smith, Analysis of Turbulent Boundary Layers, (Academic Press, New York, 1974).

6. Schlichting, H., "Boundary-Layer Theory," McGraw-Hill Book Company, 1968.

7. King, William S., "The Effect of Wall Temperature and Suction on Laminar Boundary-Layer Stability," Rand Report R-1863-ARPA, April 1976.

8. Groth, E. E. and Pfenninger, W., "Boundary Layer Transition on Bodies of Revolution," Northrop Aircraft Report NAI-57-1162 (BLC-100), July 1957.

TABLE 1. (con't)

Computed Laminar Boundary Layer Data

β	T_∞ (°F)	T_w (°F)	η_δ*	η_Θ	H	τ_c	q_c
-0.19884	60.0	60.0	2.348687	0.585424	4.011941	0.002027	0.000000
-0.19883	60.0	60.0	2.342079	0.585412	4.000732	0.003361	0.000000
-0.19882	60.0	60.0	2.337443	0.585401	3.992893	0.004303	0.000000
-0.19881	60.0	60.0	2.333660	0.585389	3.986510	0.005074	0.000000
-0.19880	60.0	60.0	2.330387	0.585378	3.980997	0.005745	0.000000
-0.19850	60.0	60.0	2.281900	0.585037	3.900435	0.015972	0.000000
-0.19750	60.0	60.0	2.210756	0.583943	3.785911	0.032011	0.000000
-0.19500	60.0	60.0	2.116816	0.581349	3.641214	0.055229	0.000000
-0.19000	60.0	60.0	2.006623	0.576511	3.480631	0.085738	0.000000
-0.18000	60.0	60.0	1.871494	0.567695	3.296658	0.128663	0.000000
-0.16000	60.0	60.0	1.706604	0.552181	3.090658	0.190800	0.000000
-0.13000	60.0	60.0	1.551150	0.532256	2.914295	0.261439	0.000000
-0.10000	60.0	60.0	1.442681	0.515027	2.801174	0.319285	0.000000
-0.05000	60.0	60.0	1.312355	0.490445	2.675848	0.400337	0.000000
0.00000	60.0	60.0	1.216777	0.469578	2.591214	0.469615	0.000000
0.05000	60.0	60.0	1.141737	0.451445	2.529073	0.531145	0.000000
0.10000	60.0	60.0	1.080322	0.435431	2.481042	0.587052	0.000000
0.20000	60.0	60.0	0.984163	0.408199	2.410986	0.686726	0.000000
0.30000	60.0	60.0	0.911000	0.385701	2.361935	0.774775	0.000000
0.40000	60.0	60.0	0.852642	0.366652	2.325477	0.854444	0.000000
0.50000	60.0	60.0	0.804557	0.350228	2.297236	0.927705	0.000000
-0.20893	60.0	90.0	2.097875	0.580306	3.615118	0.020767	19.329570
-0.20892	60.0	90.0	2.096681	0.580283	3.613205	0.021024	19.342323
-0.20890	60.0	90.0	2.094364	0.580237	3.609500	0.021525	19.367075
-0.20880	60.0	90.0	2.083930	0.580018	3.592874	0.023798	19.478611
-0.20870	60.0	90.0	2.074888	0.579813	3.578549	0.025790	19.575370
-0.20860	60.0	90.0	2.066812	0.579618	3.565818	0.027585	19.661891
-0.20850	60.0	90.0	2.059455	0.579430	3.554276	0.029236	19.740772
-0.20750	60.0	90.0	2.005769	0.577771	3.471562	0.041700	20.318500
-0.20500	60.0	90.0	1.924881	0.574273	3.351856	0.061960	21.196521
-0.20250	60.0	90.0	1.869508	0.571155	3.273209	0.076934	21.803340
-0.20000	60.0	90.0	1.825620	0.568247	3.212725	0.089487	22.287952
-0.19891	60.0	90.0	1.808807	0.567028	3.189980	0.094465	22.474502
-0.19880	60.0	90.0	1.807173	0.566906	3.187782	0.094953	22.492660
-0.19850	60.0	90.0	1.802772	0.566576	3.181873	0.096275	22.541591
-0.19750	60.0	90.0	1.788641	0.565488	3.163007	0.100562	22.698951
-0.19500	60.0	90.0	1.756391	0.562845	3.120561	0.110609	23.059513
-0.19000	60.0	90.0	1.701585	0.557833	3.050348	0.128559	23.677093
-0.18000	60.0	90.0	1.615822	0.548625	2.945222	0.159041	24.656871
-0.16000	60.0	90.0	1.493300	0.532410	2.804791	0.208316	26.089111
-0.13000	60.0	90.0	1.366991	0.511660	2.671677	0.267459	27.613670
-0.10000	60.0	90.0	1.275009	0.493801	2.582028	0.316948	28.761150
-0.05000	60.0	90.0	1.161749	0.468446	2.480004	0.386971	30.226741
0.00000	60.0	90.0	1.077358	0.447036	2.410002	0.447078	31.364421
0.05000	60.0	90.0	1.010544	0.428511	2.358267	0.500513	32.298393
0.10000	60.0	90.0	0.955591	0.412213	2.318197	0.549049	33.092254
0.20000	60.0	90.0	0.869203	0.384630	2.259846	0.635467	34.395675
0.30000	60.0	90.0	0.803296	0.361966	2.219259	0.711632	35.444625
0.40000	60.0	90.0	0.750673	0.342869	2.189386	0.780389	36.323066
0.50000	60.0	90.0	0.707308	0.326472	2.166520	0.843481	37.078964

TABLE 1. (con't)

Computed Laminar Boundary Layer Data

β	T_∞ (°F)	T_w (°F)	η_δ*	η_Θ	H	τ_c	q_c
-0.21824	60.0	120.0	1.907363	0.571916	3.335039	0.030837	43.006950
-0.21823	60.0	120.0	1.906636	0.571889	3.333927	0.030999	43.024307
-0.21822	60.0	120.0	1.905916	0.571862	3.332826	0.031160	43.041473
-0.21820	60.0	120.0	1.904495	0.571808	3.330654	0.031477	43.075386
-0.21810	60.0	120.0	1.897745	0.571547	3.320366	0.032993	43.236473
-0.21800	60.0	120.0	1.891496	0.571296	3.310883	0.034406	43.385727
-0.21750	60.0	120.0	1.865260	0.570155	3.271494	0.040451	44.013336
-0.21500	60.0	120.0	1.782535	0.565583	3.151677	0.060737	46.004394
-0.21000	60.0	120.0	1.685818	0.558277	3.019682	0.087017	48.359115
-0.20750	60.0	120.0	1.650271	0.555035	2.973271	0.097434	49.232963
-0.20500	60.0	120.0	1.619387	0.551968	2.933840	0.106842	49.996231
-0.20250	60.0	120.0	1.591915	0.549040	2.899452	0.115499	50.678520
-0.20000	60.0	120.0	1.567077	0.546228	2.868908	0.123569	51.298301
-0.19891	60.0	120.0	1.556932	0.545033	2.856582	0.126934	51.552261
-0.19880	60.0	120.0	1.555929	0.544914	2.855367	0.127269	51.577400
-0.19850	60.0	120.0	1.553212	0.544589	2.852083	0.128178	51.645500
-0.19750	60.0	120.0	1.544346	0.543514	2.841408	0.131165	51.868003
-0.19500	60.0	120.0	1.523349	0.540888	2.816386	0.138366	52.396461
-0.19000	60.0	120.0	1.485516	0.535859	2.772212	0.151803	53.354301
-0.18000	60.0	120.0	1.421936	0.526530	2.700580	0.175813	54.981666
-0.16000	60.0	120.0	1.324418	0.509994	2.596931	0.216499	57.526435
-0.13000	60.0	120.0	1.218404	0.488800	2.492641	0.266882	60.372184
-0.10000	60.0	120.0	1.138873	0.470591	2.420090	0.309670	62.572181
-0.05000	60.0	120.0	1.039121	0.444826	2.336016	0.370665	65.427765
0.00000	60.0	120.0	0.963869	0.423162	2.277779	0.423209	67.667450
0.05000	60.0	120.0	0.903895	0.404491	2.234651	0.469969	69.515762
0.10000	60.0	120.0	0.854374	0.388121	2.201307	0.512442	71.091400
0.20000	60.0	120.0	0.776284	0.360548	2.153070	0.588008	73.683960
0.30000	60.0	120.0	0.716587	0.338018	2.119970	0.654518	75.772766
0.40000	60.0	120.0	0.668893	0.319125	2.096024	0.714475	77.522247
0.50000	60.0	120.0	0.629591	0.302971	2.078055	0.769422	79.027160
-0.22432	60.0	150.0	1.668855	0.555501	3.004236	0.056513	73.543930
-0.22430	60.0	150.0	1.668331	0.555461	3.003510	0.056644	73.564636
-0.22420	60.0	150.0	1.665739	0.555261	2.999920	0.057292	73.667144
-0.22410	60.0	150.0	1.663189	0.555063	2.996397	0.057932	73.767929
-0.22400	60.0	150.0	1.660682	0.554867	2.992939	0.058563	73.867111
-0.22350	60.0	150.0	1.648716	0.553907	2.976520	0.061601	74.340744
-0.22250	60.0	150.0	1.627128	0.552083	2.947254	0.067189	75.197006
-0.22000	60.0	150.0	1.582378	0.547908	2.888035	0.079226	76.979248
-0.21500	60.0	150.0	1.514734	0.540569	2.802108	0.098662	79.694442
-0.21000	60.0	150.0	1.462634	0.534045	2.738785	0.114727	81.805389
-0.20500	60.0	150.0	1.419570	0.528060	2.688269	0.128783	83.564804
-0.20000	60.0	150.0	1.382571	0.522482	2.646161	0.141459	85.088073
-0.19750	60.0	150.0	1.365801	0.519817	2.627465	0.147396	85.782272
-0.19500	60.0	150.0	1.349986	0.517225	2.610054	0.153109	86.439193
-0.19000	60.0	150.0	1.320791	0.512238	2.578471	0.163954	87.657974
-0.18000	60.0	150.0	1.270015	0.502926	2.525252	0.183791	89.797714
-0.16000	60.0	150.0	1.188935	0.486326	2.444728	0.218285	93.273513
-0.13000	60.0	150.0	1.097691	0.465001	2.360620	0.261862	97.287094

TABLE 1. (con't)

Computed Laminar Boundary Layer Data

β	T_∞ (°F)	T_w (°F)	η_δ^*	η_Θ	H	τ_c	q_c
-0.10000	60.0	150.0	1.027770	0.446601	2.300852	0.299266	100.450226
-0.05000	60.0	150.0	0.938834	0.420846	2.230822	0.352900	104.606933
0.00000	60.0	150.0	0.871094	0.399193	2.182135	0.399247	107.893966
0.05000	60.0	150.0	0.816824	0.380597	2.146166	0.440539	110.618316
0.10000	60.0	150.0	0.771875	0.364347	2.118518	0.478057	112.946487
0.20000	60.0	150.0	0.700824	0.337094	2.079018	0.544800	116.784454
0.30000	60.0	150.0	0.646428	0.314944	2.052514	0.603514	119.880172
0.40000	60.0	150.0	0.602951	0.296456	2.033863	0.656412	122.473739
0.50000	60.0	150.0	0.567130	0.280713	2.020318	0.704865	124.704559

4 January 1979
JJE:pjk

TABLE 2.

Critical Reynolds Number Variation with Shape Factor

	$R_{\delta^*_{crit}}$	H
1	105.000	3.80000
2	115.000	3.50000
3	130.000	3.20000
4	150.000	3.00000
5	180.000	2.90000
6	232.000	2.80000
7	326.000	2.70000
8	485.000	2.60000
9	675.000	2.55000
10	1000.000	2.51800
11	1500.000	2.48750
12	2000.000	2.46600
13	3000.000	2.43750
14	4000.000	2.41800
15	5000.000	2.40250
16	6000.000	2.38950
17	7000.000	2.37550
18	8000.000	2.36050
19	9000.000	2.34400
20	10000.000	2.32540
21	10500.000	2.31500
22	11000.000	2.29750
23	11210.000	2.28000

4 January 1979
JJE:pjk

Table 3

Comparison of Laminar Separation Results

for Two-Dimensional Unheated Case

f''_w (ARL)	f''_w (Keller-Cebeci), (Smith)	β (ARL)	β (Keller-Cebeci)	β (Smith)
+.00064472 -.00076458	0	-.19891	-.20259	-.198838
.0551894	.05517	-.195	-.19528	-.195
.0857052	.08570	-.190	-.19023	-.190
.128638	.12864	-.180	-.18025	-.180
.190780	.19078	-.160	-.16016	-.160
.239736	.23974	-.140	-.14024	-.140
.319270	.31927	-.100	-.10017	-.100
.400322	.40032	-.050	-.05031	-.050
.469600	.46960	0	-.00031	0

TABLE 4.

Transition Reynolds Number Variation with Shape Factor

H	$R_{x_{trans}}$	$\log_{10}[R_{x_{trans}}]$
2.20000	8.51732	0.32909E 09
2.25000	8.28045	0.19074E 09
2.30000	8.04405	0.11067E 09
2.35000	7.80882	0.64390E 08
2.40000	7.57548	0.37625E 08
2.45000	7.34473	0.22117E 08
2.50000	7.11730	0.13100E 08
2.55000	6.89390	0.78324E 07
2.60000	6.67524	0.47341E 07
2.65000	6.46204	0.28976E 07
2.70000	6.25501	0.17989E 07
2.75000	6.05486	0.11346E 07
2.80000	5.86231	0.72829E 06
2.84999	5.67808	0.47651E 06
2.90000	5.50287	0.31832E 06
2.95000	5.33741	0.21747E 06

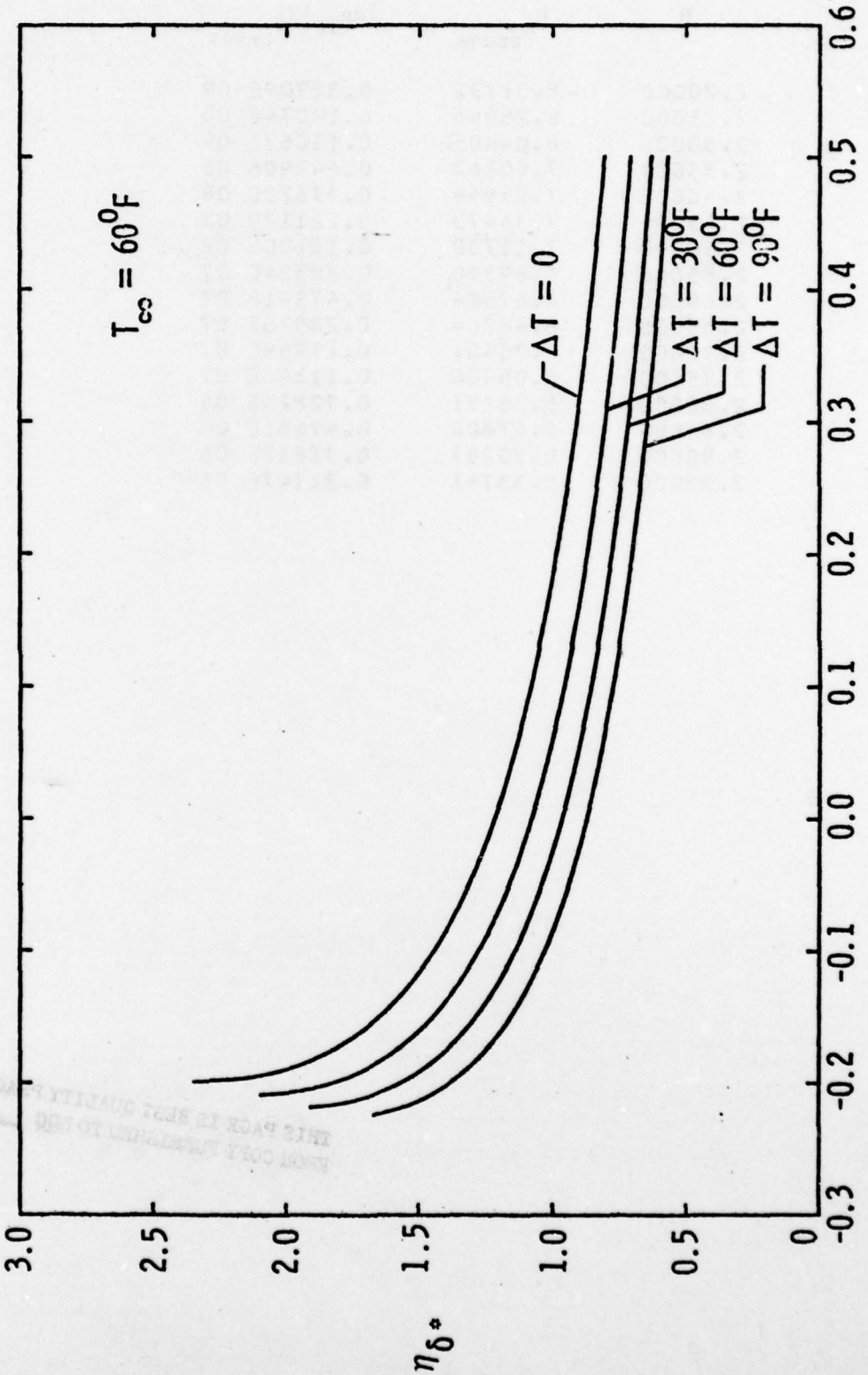

Figure 1 - Variation of η_{δ^*} with β Parameter

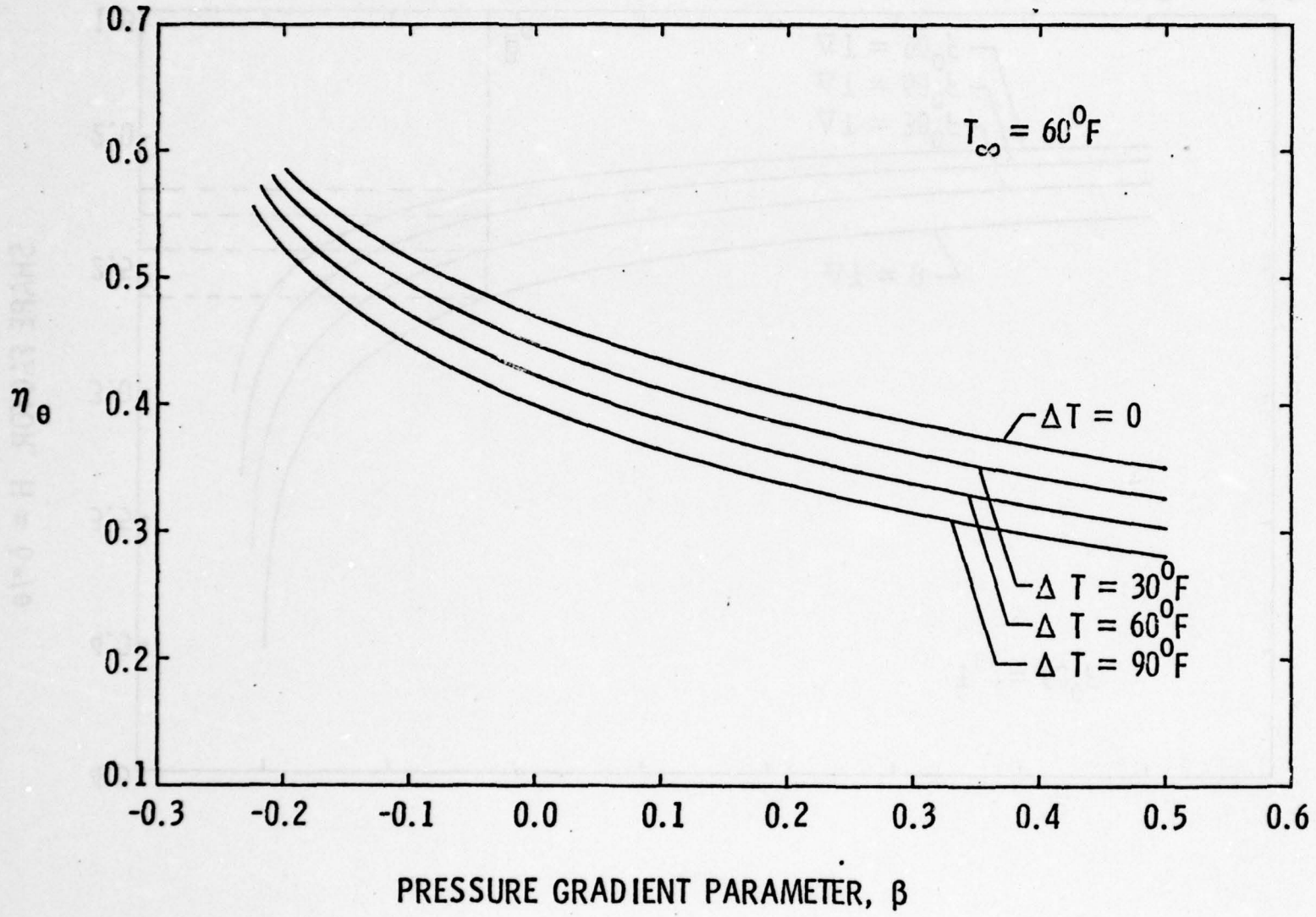

Figure 2 - Variation of η_θ with β Parameter

4 January 1979
JJE:pjk

4 January 1979
JJE:pjk

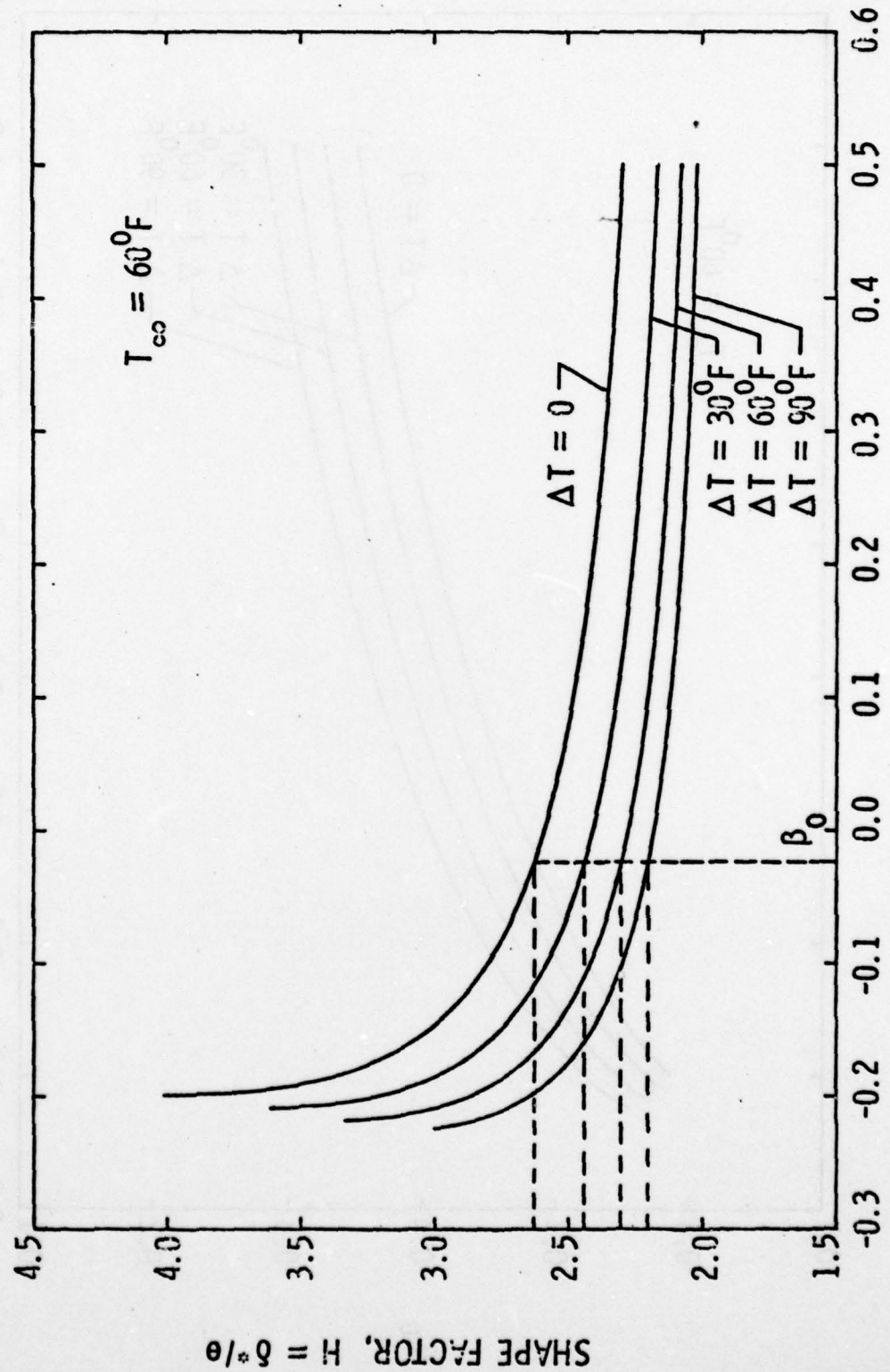

Figure 3 - Shape Factor Variation with β Parameter

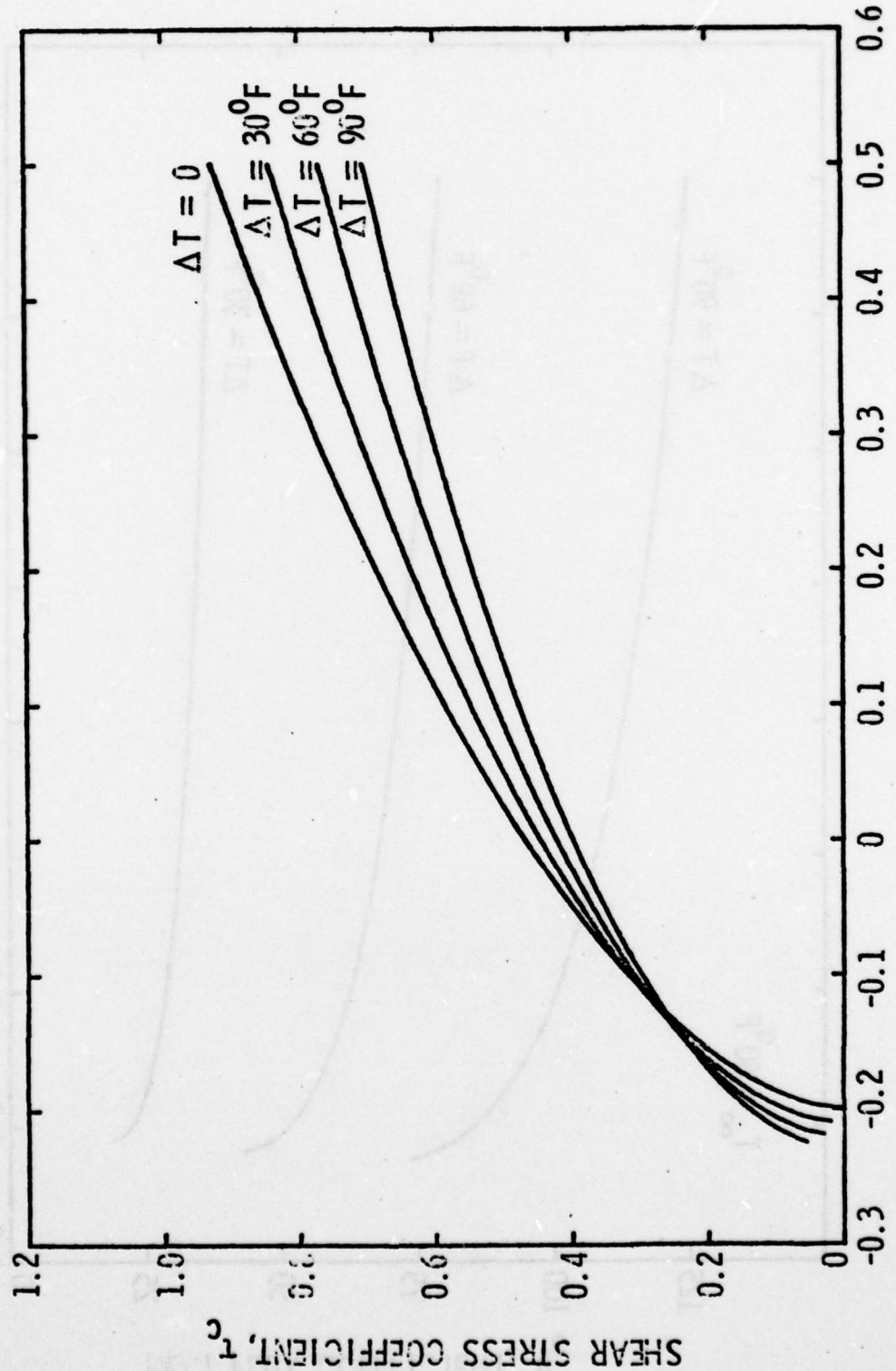

Figure 4 - Variation of τ_c with β Parameter

4 January 1979
JJE:pjk

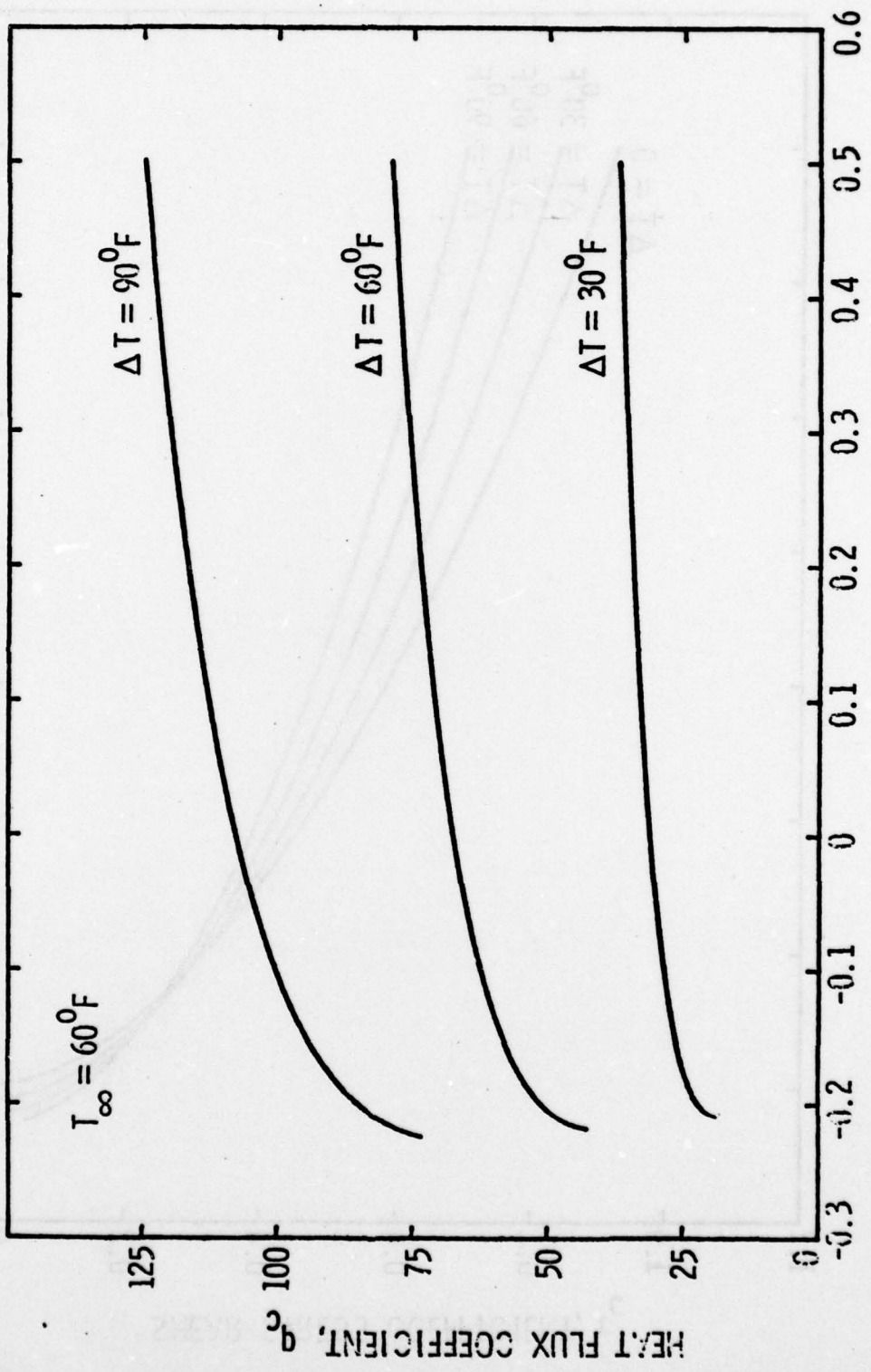

Figure 5 - Variation of q_c with β Parameter

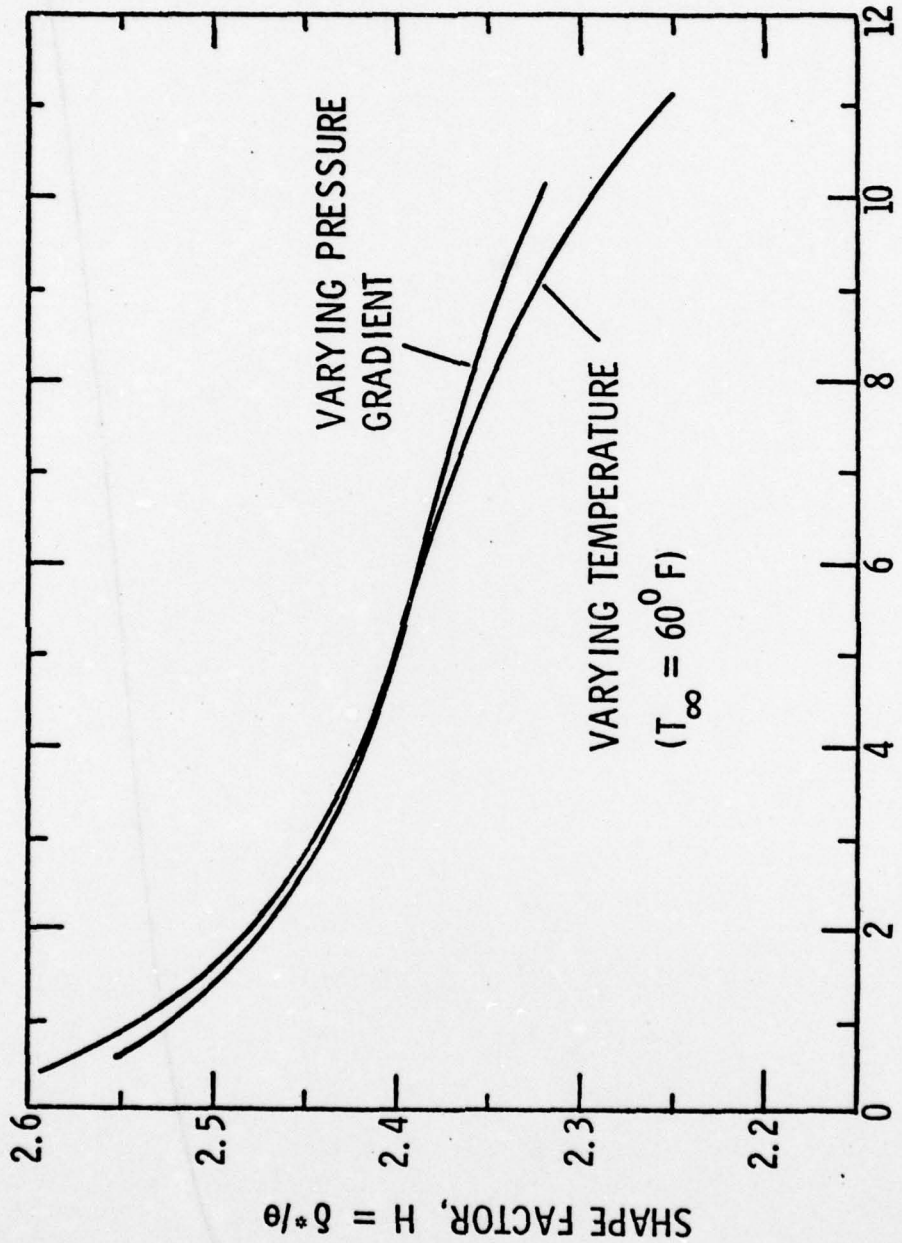

Figure 6 - Correlation of Shape Factor with Critical Reynolds number

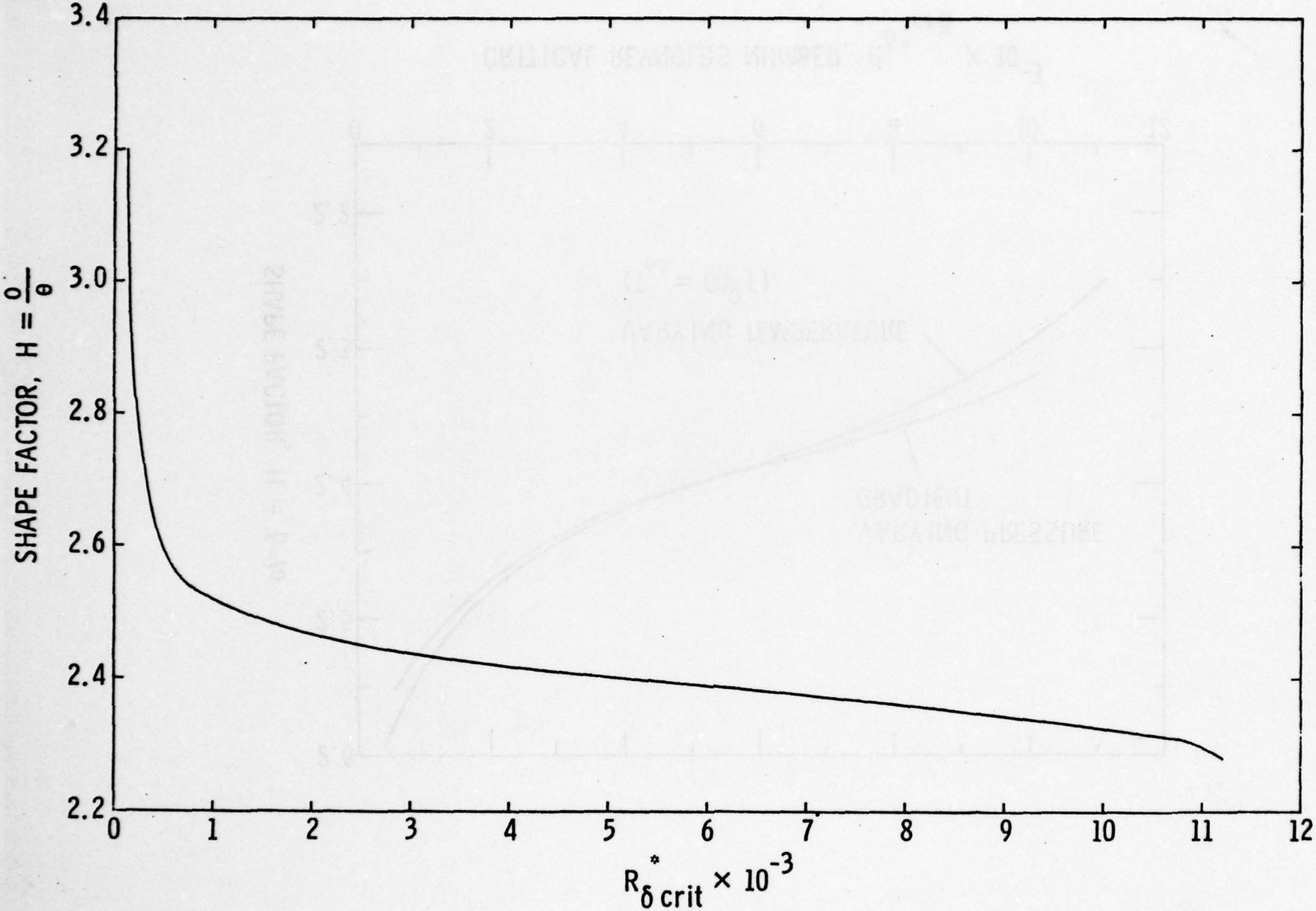

Figure 7 - Shape Factor vs Critical Reynolds number

4 January 1979
JJE:pjk

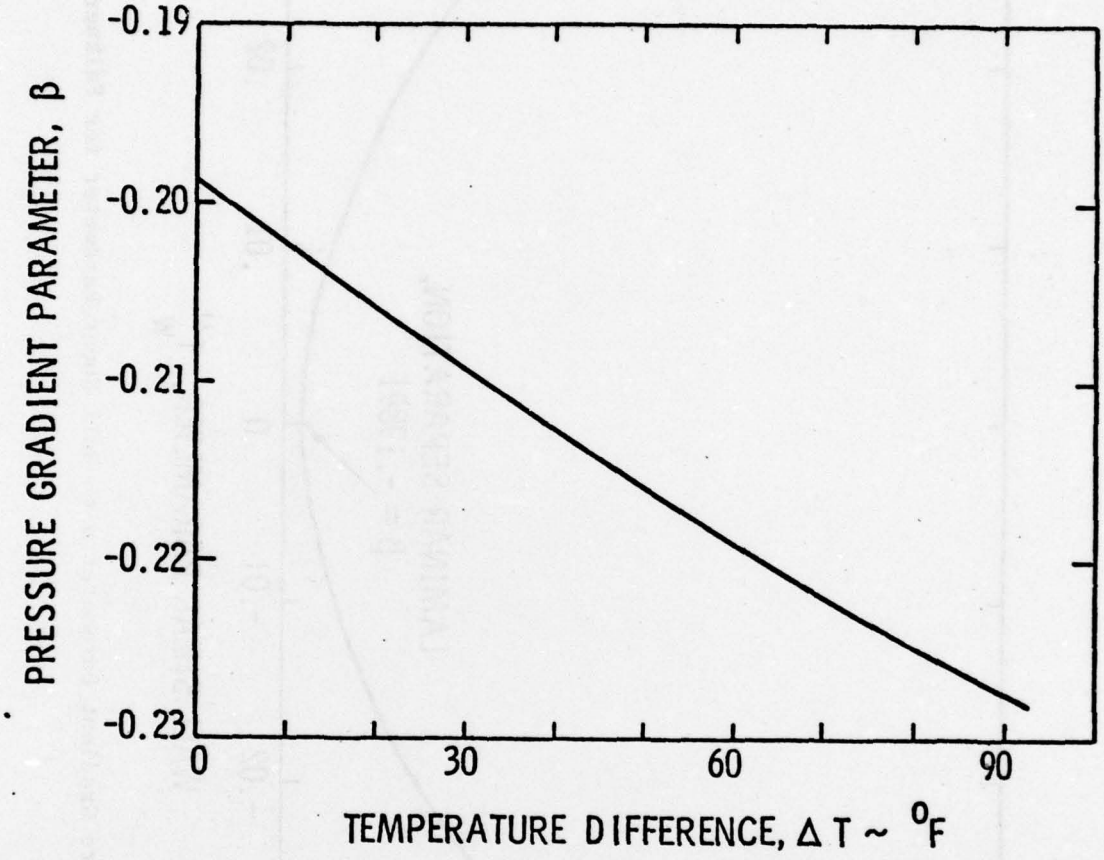

Figure 8 - Laminar Separation Limit Curve

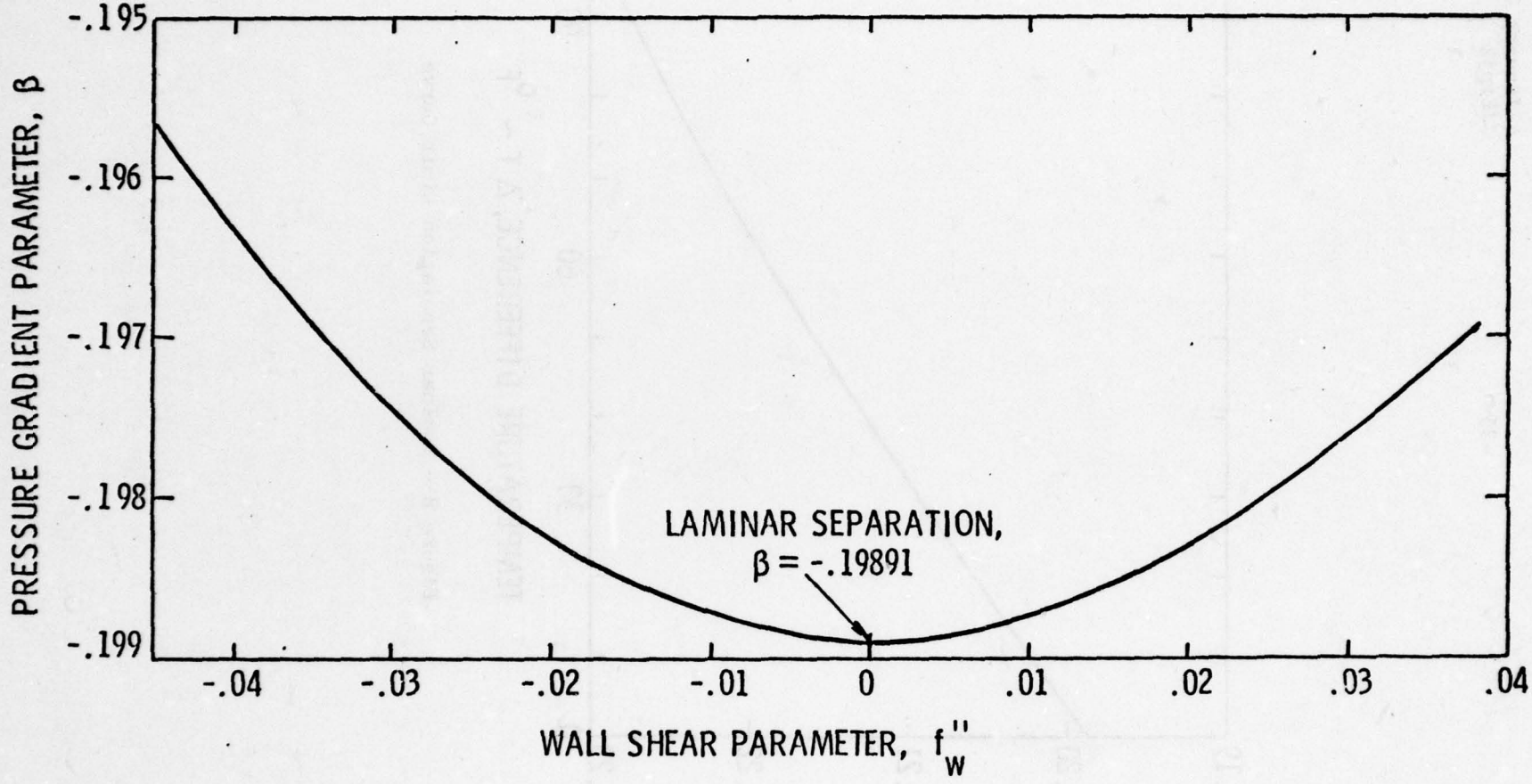

Figure 9 - Variation of Pressure Gradient Parameter with Wall Shear Parameter for Falkner - Skan Flows

4 January 1979
JJE:pjk

4 January 1979
JJE:pjk

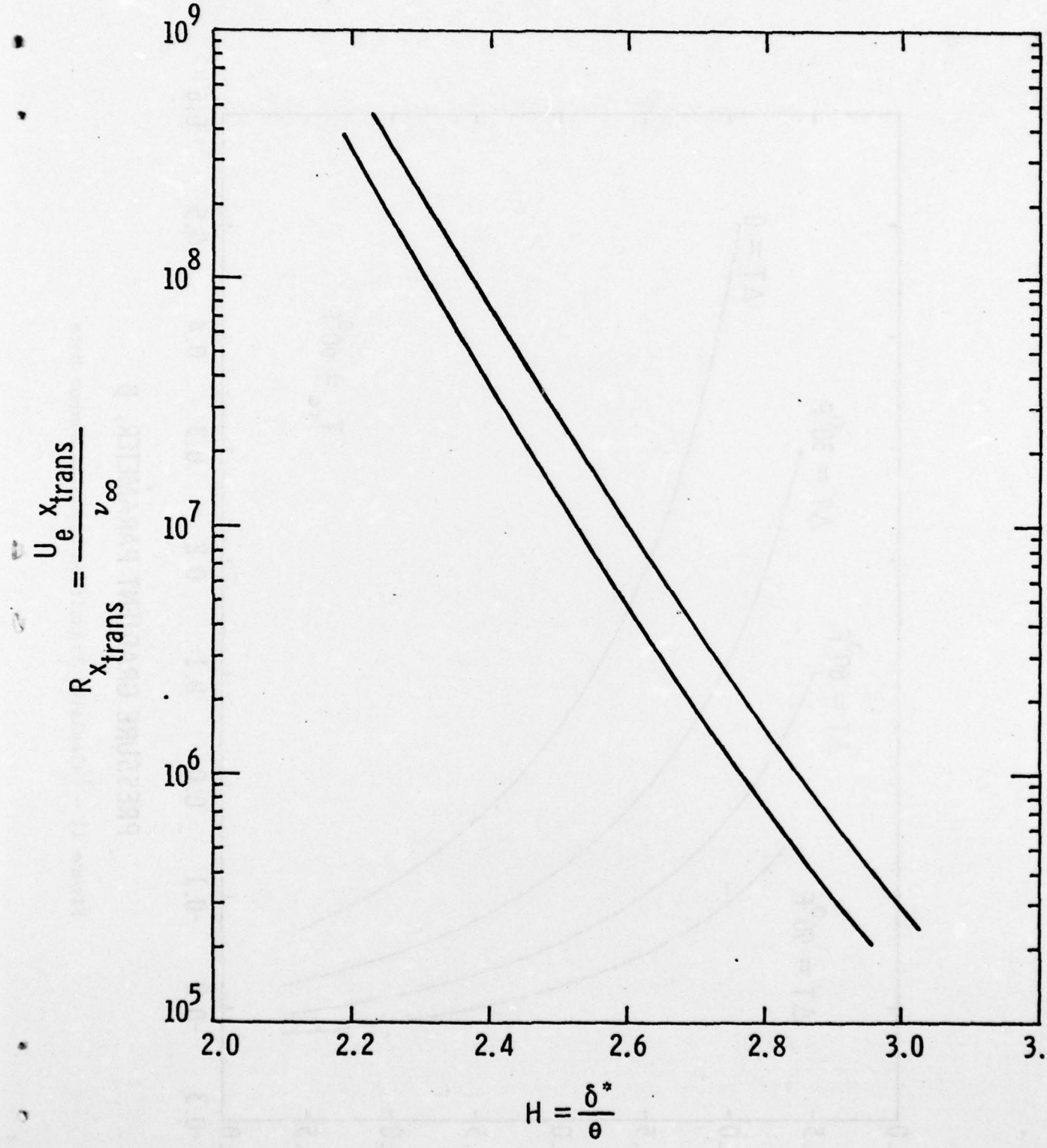

Figure 10 - Transition Reynolds Number Variation with H from e^9 Stability Calculations

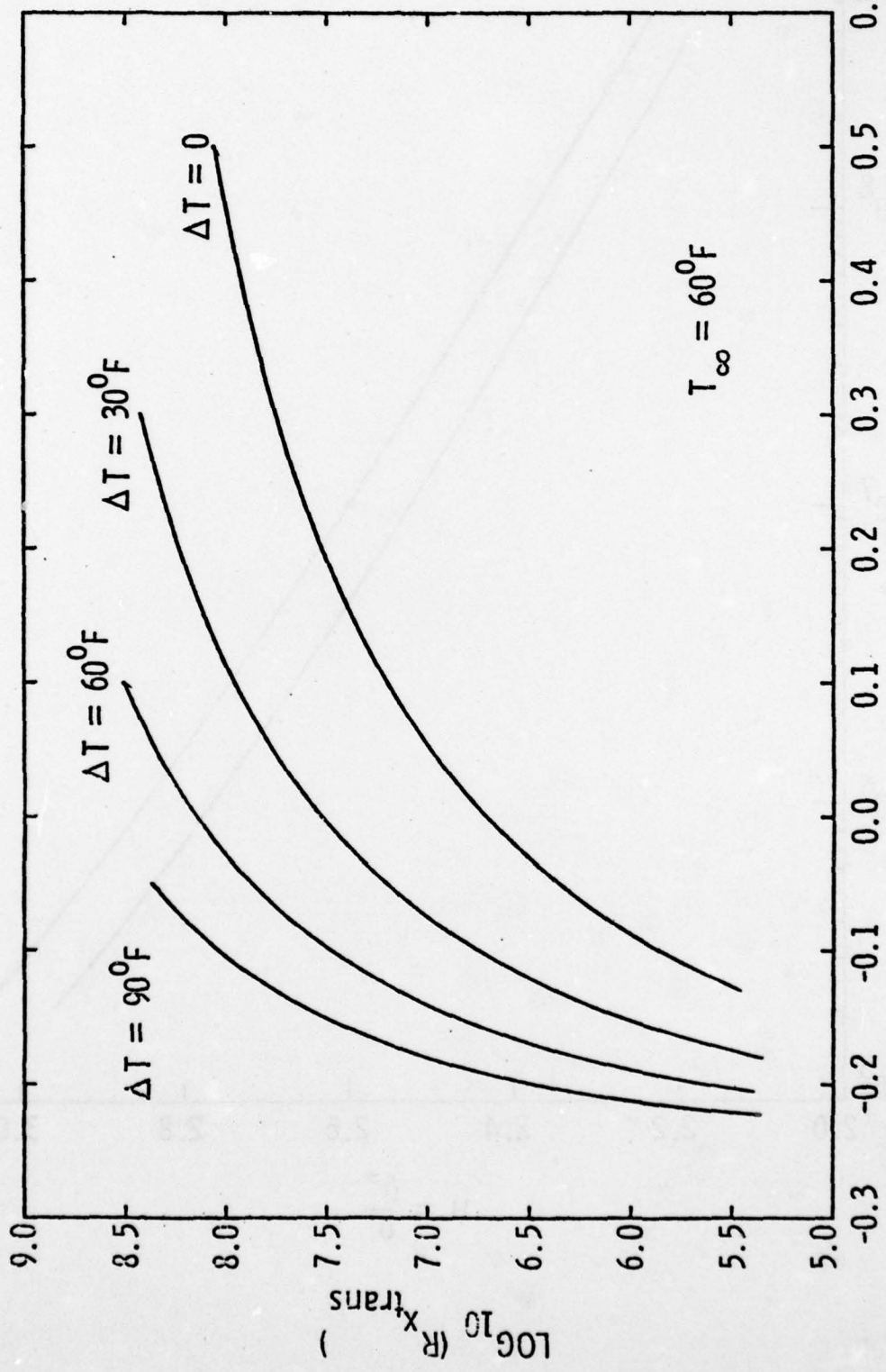

Figure 11 - Calculated Transition Reynolds Number Data

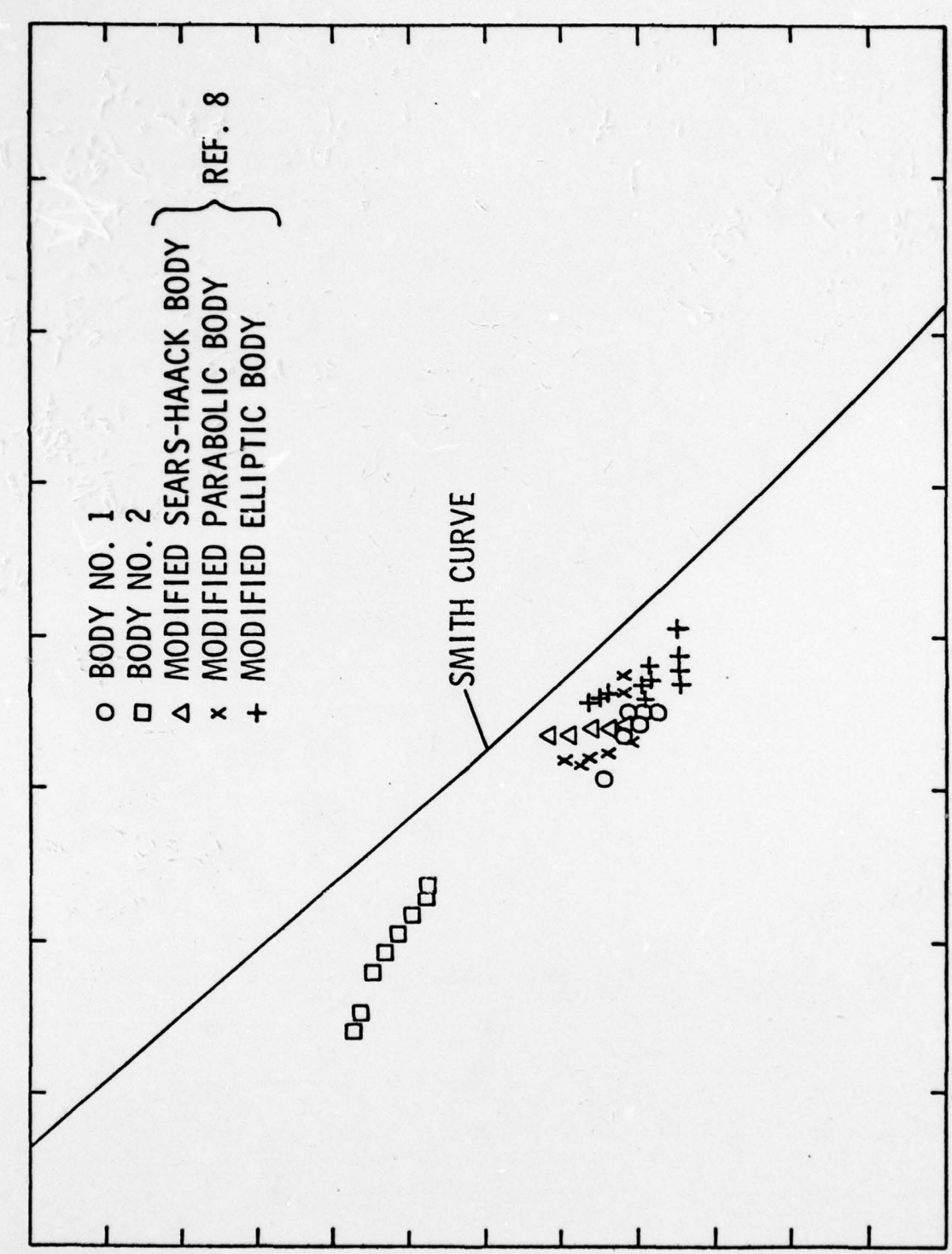

Figure 12 - Log Plot of Transition Reynolds Number Variation with Shape Factor

DISTRIBUTION LIST FOR UNCLASSIFIED TM 79-02 by J. J. Eisenhuth and G. H. Hoffman, dated 01/04/79.

Commander
Naval Sea Systems Command
Department of the Navy
Washington, DC 20362
Attn: Library
Code NSEA-09G32
(copy Nos. 1 and 2)

Naval Sea Systems Command
Attn: C. G. McGuigan
Code NSEA-03133
(Copy No. 3)

Naval Sea Systems Command
Attn: L. Benen
Code NSEA-0342
(Copy No. 4)

Naval Sea Systems Command
Attn: E. G. Liszka
Code NSEA-0342
(Copy No. 5)

Naval Sea Systems Command
Attn: G. Sorkin
Code NSEA-035
(Copy No. 6)

Naval Sea Systems Command
Attn: T. E. Peirce
Code NSEA-0351
(Copy No. 7)

Commanding Officer
Naval Underwater Systems Center
Newport, RI 02840
Attn: D. Goodrich
Code SB323
(Copy No. 8)

Naval Underwater Systems Center
Attn: R. Nadolink
Code SB323
(Copy No. 9)

Naval Underwater Systems Center
Attn: R. Trainor
Code SB323
(Copy No. 10)

Naval Underwater Systems Center
Attn: Library
Code LA15
(Copy No. 11)

Commanding Officer
Naval Ocean Systems Center
San Diego, CA 92152
Attn: J. W. Hoyt
Code 2501
(Copy No. 12)

Naval Ocean Systems Center
Attn: D. Nelson
Code 2542
(Copy No. 13)

Naval Ocean Systems Center
Attn: A. G. Fabula
Code 5311
(Copy No. 14)

Commander
David W. Taylor Naval Ship R&D Center
Department of the Navy
Bethesda, MD 20084
Attn: Tech. Info. Lib.
(Copy No. 15)

David W. Taylor Naval Ship R&D Center
Attn: W. E. Cummins
Code 15
(Copy No. 16)

David W. Taylor Naval Ship R&D Center
Attn: S. F. Crump
Code 1505
(Copy No. 17)

David W. Taylor Naval Ship R&D Center
Attn: J. McCarthy
Code 1552
(Copy No. 18)

David W. Taylor Naval Ship R&D Center
Attn: M. Sevik
Code 19
(Copy No. 19)

DISTRIBUTION LIST FOR UNCLASSIFIED TM 79-02 by J. J. Eisenhuth and G. H. Hoffman, dated 01/04/79.

David W. Taylor Naval Ship R&D Center
Attn: P. S. Granville
(Copy No. 20)

Office of Naval Research
Department of the Navy
800 N. Quincy Street
Arlington, VA 22217
Attn: Ralph Cooper
(Copy No. 21)

Defense Documentation Center
5010 Duke Street
Cameron Station
Alexandria, VA 22314
(Copy Nos. 22 - 33)

National Bureau of Standards
Aerodynamics Section
Washington, DC 20234
Attn: P. S. Klebanoff
(Copy No. 34)

Rand Corporation
1700 Main Street
Santa Monica, CA 90406
Attn: R. King
(Copy No. 35)

Rand Corporation
Attn: C. Gazley
(Copy No. 35)

Jet Propulsion Laboratory
Pasadena, CA 01109
Attn: L. Mack
(Copy No. 37)

Applied Research Laboratory
P. O. Box 30
State College, PA 16801
Attn: J. J. Eisenhuth
(Copy No. 38)

Applied Research Laboratory
Attn: G. H. Hoffman
(Copy No. 39)

GTWT Files
Applied Research Laboratory
(Copy No. 40)